







Framework for Strain Measurements at Cyclic Loaded Structures with Planar Elastoresistive Sensors Applying Electrical Impedance Tomography

Jonas Wagner^(✉), Christoph Kralovec, Daniel Kimpfbeck,
Lukas Heinzlmeier, and Martin Schagerl

Institute of Structural Lightweight Design, Johannes Kepler University Linz,
Linz, Austria
jonas.wagner@jku.at
<http://jku.at/ikl>

Abstract. In the field of Structural Health Monitoring (SHM), strain is an often-used parameter for the evaluation of the structural integrity. A rather new approach to efficiently monitor the global strain field of a mechanical structure is to employ planar elastoresistive sensors as surface coating in combination with Electrical Impedance Tomography (EIT). Furthermore, the EIT approach simultaneously allows the monitoring for damages of the sensor area. The aim of this experimental research is the evaluation of homogeneous strain states under cyclic loading using planar elastoresistive sensors applying EIT. The purpose is to develop an experimental framework that involves various methods for strain evaluation (e.g., EIT, Montgomery method, strain gauge) in order to have a suitable test setup for new EIT evaluation methods and sensor material properties (e.g., set-in effect) including long-term behavior. In the future, this framework shall allow the investigation and improvement of EIT reconstruction for non-static loaded structures. In the present study, the considered specimen is a cyclic loaded tensile test coupon. For this first investigation, static load steps discretize the cyclic loading. Additional strain measurement methods, such as a traditional strain gauge, are applied for validation.

Keywords: Electrical Impedance Tomography · EIT · Structural Health Monitoring · SHM · Strain sensor · Long-term cyclic loading

1 Introduction

Lightweight design aims to enable mechanical structures and their components to be as light as possible while preserving their underlying function. Due to uncertainties in the structural design, this may involve the assessment of the considered structure's integrity by monitoring the amount of damage to the structure. One possibility is to perform periodic inspections, which are usually cost-intensive. In aviation, this procedure is state-of-the-art. An alternative

may be the permanent monitoring of vulnerable structures during operation with online systems of sensors. This is known as Structural health monitoring (SHM). The basic idea of SHM is that, on the one hand, the absence of damage in a structure can be stated at any time or, on the other hand, the size of the damage can be permanently monitored until reaching a critical size [12]. Nowadays, a wide variety of methods are considered for SHM. Some well-known methods are piezoelectric-sensor-based monitoring methods (e.g. guided waves) [7, 16, 22] or strain-based monitoring methods [4, 11]. A rather recent method for continuous monitoring is the Electrical Impedance Tomography (EIT) combined with electrically conductive structures or thin-film surface sensors. EIT, which originated from medical technology, enables loads and condition monitoring of larger areas by reconstructing spatial conductivities or conductivity changes by voltage potential measurements at the boundary. For this purpose, several electrodes are placed around an area that is to be monitored in the context of SHM. Due to systematically injecting current between these electrodes, the required measurement data is obtained by measuring the voltages between the remaining electrodes. With these discrete measurement data, insights into the conductivity change in the region of interest can be gained by the inverse reconstruction of the EIT. Thereby, an electrically conductive structure itself can serve as the sensor material. This is referred to as self-sensing materials. Components and structures that fulfill these characteristics are typically made of carbon-fiber reinforced polymers (CFRP) [10, 18, 20]. Metallic structures itself are only suitable to a limited extent, since their good conductivity results in very low electrode voltages, which requires special and even more complex measurement setups [15]. A further approach is the application of a conductive planar sensor thin-film to a specific area of the structure of interest [13, 14, 24]. This has the benefit of being independent of the electrical nature of the structure under investigation, given that the sensor is electrically isolated from it. Moreover the sensor materials have advantageous properties and can be tailored to the application, e.g., by utilizing the elastoresistive behavior of an applied conductive sensor thin-film, it is also possible to evaluate the conductivity change based on strain [21, 23]. This allows the strain field to be monitored over the entire sensor surface. However, operational loads are typically not static, and furthermore, electrical properties of sensor materials change due to mechanical loading [6].

This work presents a framework for the experimental investigation of these issues. The framework shall allow (i), voltage measurements for EIT at planar elastoresistive sensors applied to cyclic and dynamically loaded structures, and (ii), the investigation of the sensor material's electrical properties when subjected to cyclic loading. The latter, so-called set-in effect, is little investigated for larger numbers of load cycles and used to present the potential of the proposed experimental framework by a case example. The considered case example is a cyclic loaded tensile test coupon equipped with a planar elastoresistive thin-film sensor made of carbon paste. For this exemplary sensor material, the conductivity change in the unstrained state will be investigated over nearly 1.5 million load cycles. Furthermore, the elastoresistive behavior of the used planar sensor in

relation to the number of load cycles is to be analyzed. In this context, the EIT and the Montgomery method are used to determine the conductivity and the conductivity change.

2 Fundamentals

For the measurement of the conductivity or conductivity change, two measurement methods are used in the further progress of this paper. Apart from the aforementioned EIT, the Montgomery method is used as a second conductivity evaluation method to support findings. This is possible, since we consider a homogeneous strain, and thus, conductivity field, and furthermore, voltage potential measurements required for EIT also allow the derivation of the required measurements for the Montgomery method.

2.1 EIT

The EIT is an imaging method originating from medical technology that deals with conductivity or conductivity changes inside a defined area of interest. Therefore, several electrodes are placed around the electrically conductive domain Ω to be monitored. By injecting current between two electrodes, and thus, through the domain Ω , an electric field is generated. Simultaneous voltage difference measurements on adjacent pairs of the remaining electrodes provide the voltage measurement data required. In EIT, a distinction is made between absolute and differential EIT. In absolute EIT, an estimate of the spatial conductivity is calculated from a single set of voltage measurement data. In the case of differential EIT, two independent voltage measurement data sets are used and the conductivity change in the domain Ω is calculated from them. The differential EIT has the advantage that it is more robust, against deviations of the underlying EIT model to the real sensor and measurement noise, than the absolute EIT [8]. For this reason, a 2D differential EIT approach is chosen for this study.

Furthermore, the EIT distinguishes the respective solution direction. In the so-called forward problem

$$\mathbf{H}\boldsymbol{\sigma} = \mathbf{v}, \tag{1}$$

the voltages \mathbf{v} at the electrodes are calculated for a known conductivity distribution $\boldsymbol{\sigma}$ with the sensitivity matrix \mathbf{H} . Thereby, the forward problem in Eq. (1) is a linear system of equations. Thus, the forward problem is often used for simulations to obtain voltage measurement data. However, the main focus of the EIT is on solving the inverse problem. Thereby, the conductivity change inside an area of interest is reconstructed by the use of voltage measurement data sets. As a result of the circumstance that the forward problem in Eq. (1) is over-determined, a pseudo-inverse matrix \mathbf{R} must be formed from the sensitivity matrix \mathbf{H} . This allows the reconstruction of the estimated conductivity distribution $\hat{\boldsymbol{\sigma}}$ inside the domain Ω according to

$$\hat{\boldsymbol{\sigma}} = \mathbf{R}\mathbf{v}. \tag{2}$$

However, the equation system in Eq. (2) is ill-posed because the number of independent voltage measurements at the electrodes is limited. Therefore, regularization is used to solve the inverse problem of EIT. There are numerous approaches. In the present work the often used maximum *a posteriori* (MAP) regularization approach is utilized. The Gauss-Newton one-step algorithm is used to solve the inverse EIT problem [1, 2, 5]. Thus, the ill-posed mathematical problem from Eq. (3) becomes the following linear system of equations

$$\Delta\hat{\sigma} = (\mathbf{H}^T\mathbf{W}\mathbf{H} + \lambda\mathbf{Q})^{-1} (\mathbf{H}^T\mathbf{W}) \Delta\mathbf{v}. \tag{3}$$

Thereby, the matrix \mathbf{Q} represents the regularization matrix and the hyperparameter λ controls the impact of the regularization. In addition, the matrix \mathbf{W} operates as a weight matrix. Since the Gauss-Newton one-step algorithm is used to solve the differential EIT, an estimated conductivity change $\Delta\hat{\sigma}$ is reconstructed from the change in boundary voltage potentials $\Delta\mathbf{v}$.

2.2 Montgomery Method

The Montgomery method is used to calculate the conductivity or the conductivity change. The method originally presented by Montgomery [17] requires resistance measurements, at the corners of a considered rectangular electrically conductive area. In the present experimental measurements, these were not acquired directly but calculated from the measurements required for EIT. Figure 1 shows the obtaining of the measurement data for the Montgomery method from the EIT data, e.g., for the required measurement data in y-direction R_y , the 6th current path i_6 and the voltage measurement points u_{66} - u_{69} for the implemented EIT current injection and voltage measurement pattern are used. In x-direction the same procedure is used. Due to the availability of the necessary measurement data, the revised Montgomery method by

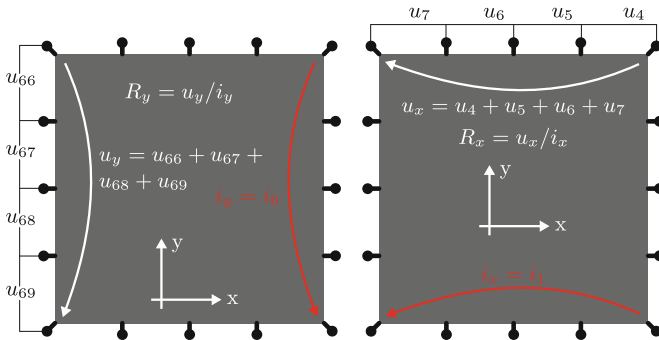


Fig. 1. Calculation of the measurement data for the Montgomery method from the implemented EIT current injection and voltage measurement pattern with 16 electrodes.

dos Santos *et al.* [19] allows the calculation of a homogeneous and isotropic equivalent sensor model with the aspect ratio

$$\frac{L_y}{L_x} \cong \frac{1}{2} \left(\frac{1}{\pi} \ln \frac{R_y}{R_x} + \sqrt{\left(\frac{1}{\pi} \ln \frac{R_y}{R_x} \right)^2 + 4} \right) \tag{4}$$

and the associated isotropic resistivity (and conductivity with $\sigma = 1/\rho$)

$$\rho = \frac{\pi}{8} L_z R_x \sinh \left(\pi \frac{L_y}{L_x} \right), \tag{5}$$

which is suitable as a comparison value for the EIT [21]. Thereby, L_z represents the planar sensor thin-film thickness.

3 Experimental Framework

In this study, the behavior of the unstrained conductivity of the sensor as well as the elastoresistive behavior of the conductive sensor thin-film with respect to cyclic loading is investigated. Therefore, a framework was developed for this purpose, which is qualified for further studies. A test rig from Zwick Roell equipped with a 25 kN cylinder is used for cyclic loading. The uni-axial tensile test is used, since a simple homogeneous strain state is present in this case. The measurement setup consists of two *HBM QuantumX MX840B* for simultaneous voltage measurement, a *Keithley 6620* current source and a switch [9, 21]. Figure 2 illustrates the complete framework used. The evaluation of the EIT data is accomplished

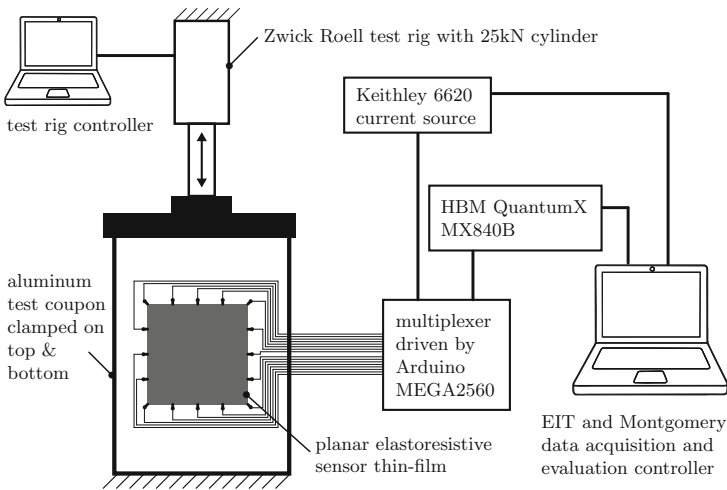


Fig. 2. Schematic illustration of the framework for EIT voltage measurements under cyclic loading.

with the open-source software EIDORS [3] and MATLAB[®] as control and analysis software. Thereby, the measurement and evaluation is fully automatic.

Anodized aluminum is used as test specimen because the sensor thin-film and the electrodes must be electrically isolated from the aluminum. Furthermore, the insulating layer must be partially resistant to solvents in order to stay isolated while attaching the electrodes to the test specimen. The anodized layer fulfills all these properties. Figure 3 shows the test specimen used in the further course of this work, with elastoresistive sensor, temperature sensor and strain gauge applied. Furthermore, a screen-printed carbon paste thin-film with a size of 30 mm × 30 mm and an average thickness of 10 μm is used as the elastoresistive planar sensor thin-film.

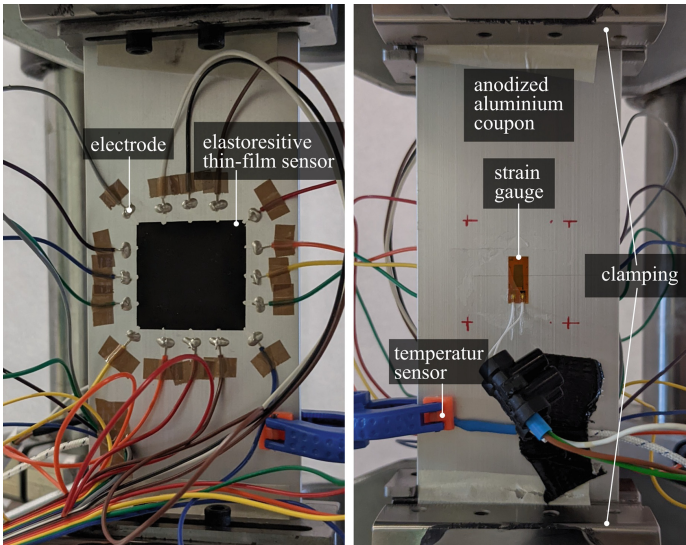


Fig. 3. Anodized aluminum coupon as test specimen for cyclic loading with the applied planar elastoresistive sensor, a temperature sensor and a strain gauge from both sides.

A characteristic of EIT is that a static load case must be maintained for the duration of the required voltage measurement. In order to investigate the behavior of the planar elastoresistive sensor thin-film as a function of the load cycles, a static load scheme is introduced that is repeatedly run through after a specified number of load cycles. This static load scheme is displayed in Fig. 4.a and contains seven measurement points at different load levels. In addition, the time periods for the EIT are marked. For better controllability of the cyclic loading, the lower load limit is set to 250 N and is assumed to be the unstrained state or the initial state. At the beginning of the cyclic load study, a significant conductivity change of the sensor can be expected (also referred to as set-in effect [6]), therefore, initially the static load scheme is repeated 10 times. The set-in

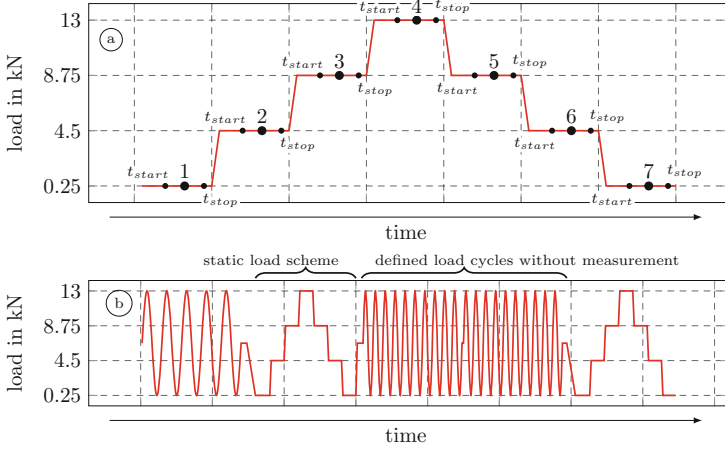


Fig. 4. (a) illustrates the static load scheme with measurements at seven load levels of a load cycle over time; t_{start} and t_{stop} mark the time of each EIT measurement. (b) illustrates a cutout of the cyclic load for the test coupon including static load schemes and defined load cycles without measurement.

effect is generally defined as the time or number of load cycles required to reach a stable state. After that, the number of cycles between the load scheme measurement is increased continuously. Figure 4.b illustrates a cutout of the applied cyclic loading for the coupon shown in Fig. 3. The sequence is thereby always the same. After a defined number of cycles without measurements, the static load scheme (cf. Fig. 4.a) is applied to investigate the elastoresistive behavior of the sensor thin-film. The number of load cycles between these measurements is specified in Table 1.

Table 1. Number of cyclic loads between the static load scheme measurements including the number of repeats in the applied order from left to right.

Load cycles	1	15	20	25	50	100	200	250	500	$1 \cdot 10^3$	$2.5 \cdot 10^3$	$5 \cdot 10^3$	$1 \cdot 10^4$	$2.5 \cdot 10^4$	$5 \cdot 10^4$	$1 \cdot 10^5$
Number of repeats	10	1	1	1	1	1	1	1	1	1	1	1	1	1	1	14

The opposite injection pattern is used to measure the EIT. For the reconstruction, the hyperparameter is determined according to the procedure presented in Wagner *et al.* [21]. The applied prior is the Laplace prior.

4 Experimental Results

For the initial experiments on the previously described framework, the test specimen shown in Fig. 3 is loaded with nearly 1.5 million load cycles between 250 N

and 13 kN. Thereby, a maximum principal normal strain of about $1110 \mu\text{m/m}$ occurs, whereas the measurements by the applied strain gauge revealed a change of the maximum principal normal strain of about 1%, so that this change is not taken into account in the following. The duration of the complete 1.5 million load cycles and the static load scheme measurements is about 44 h. The behavior of the conductivity and the elastoresistive behavior is monitored with the EIT and Montgomery method. Figure 5 shows the behavior of the conductivity in the unstrained state as a function of the number of load cycles for this experiment. Since differential EIT provides only conductivity changes ($\Delta\sigma_{i,\text{EIT}}$), the first Montgomery measurement is used as the unstrained conductivity ($\sigma_{1,\text{Mont}}$) for better illustration and to obtain absolute conductivities ($\sigma_{i,\text{EIT}} = \sigma_{1,\text{Mont}} + \Delta\sigma_{i,\text{EIT}}$). The set-in effect mentioned earlier is clearly visible by the significant conductivity increase during the first load cycles. Thereafter, the conductivity varies by less than 2% in the unstrained state, while scattering also occurs. Furthermore, a dependence of the conductivity of the sensor to temperature or humidity is not clearly evident, as can be seen in Fig. 5. On the basis of this data set, dependence can of course not be ruled out and requires further investigations. It should also be noted that the sensor material and the sensor electrodes have survived the 1.5 million load cycles, and thus, qualify for further studies in this direction.

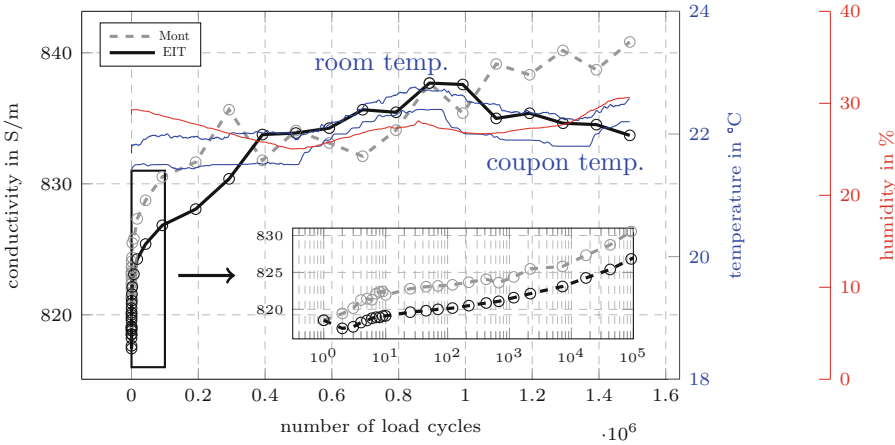


Fig. 5. Conductivity of the planar elastoresistive sensor measured with the EIT and Montgomery method in an unstrained state over number of previous loadings, overlaid by the room and the coupon temperature and the humidity during the experiment.

For investigation of the elastoresistive behavior, the static load scheme introduced in Sect. 3 is repeated after the number of cycles defined in Table 1. The first measurement is always taken as a reference measurement in the unstrained state and the change in elastoresistive behavior is analyzed. Figure 6 presents

this study evaluated with the EIT (Fig. 6.a) and with the Montgomery method (Fig. 6.b). It can be seen that there is a scattering of elastoresistive behavior (gray lines). In order to characterize this scatter, the mean absolute error is determined with respect to the stable elastoresistive behavior after the set-in effect in Fig. 6.c and Fig. 6.d. These show a stable elastoresistive behavior in a range of 10^1 to 10^5 load cycles. After that, a scattering of the elastoresistive behavior starts. However, the elastoresistive behavior repeatedly returns back to the stable behavior with increasing number of load cycles. In this context, the EIT as well as the Montgomery method provide similar results. Why the scattering of the elastoresistive behavior occurs after 10^5 load cycles or where this behavior comes from is not known at present and will be the subject of further research.

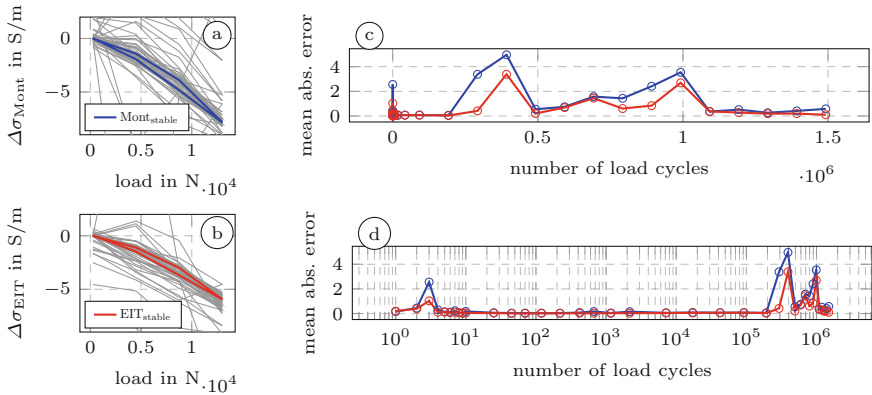


Fig. 6. Elastoresistive behavior of the conductive sensor measured by the EIT and Montgomery methods (gray lines) including the average absolute error relative to the stable elastoresistive behavior by EIT (red) and Montgomery method (blue).

5 Conclusions and Outlook

A framework for the experimental investigation of (i), voltage measurements for EIT at planar elastoresistive sensors applied to cyclic and dynamically loaded structures, and (ii), the investigation of the sensor material’s electrical properties when subjected to a large number of cyclic loads, is presented. The potential of the proposed experimental framework is demonstrated by the exemplary analysis of the electrical properties of a planar elastoresistive thin-film sensor when subjected to long-term cyclic loading. The measurement results obtained with the introduced framework show that the sensor including the sensor thin-film and contacting electrodes resist significant strains for 1.5 million load cycles, i.e., enables condition and loads monitoring at, e.g., aerospace structures. Furthermore, the proposed framework showed that the conductivity change in the

unstrained state is less than 2% after a set-in effect. This applies to over 90% of the load cycles of the sensor. Moreover, this indicates that the material used behaves reasonably stable even under a high number of load cycles. Investigation of the elastoresistive behavior revealed that after a set-in effect of the elastoresistive sensor material until about 10 load cycles, the sensor exhibits stable behavior up to a load cycle number of 10^5 . At further loading the elastoresistive behavior of the considered thin-film sensor scattered. In conclusion, apart from minor deviations, EIT and the Montgomery method achieve similar results in this research. Another interesting aspect is that the set-in effects of conductivity in the unstrained state and elastoresistive behavior have different cycle loads. This suggests that these two effects are not directly dependent on each other. However, the experimental framework passed through this high number of load cycles without any errors. This forms a good foundation for future investigations.

Future research work enabled by the proposed experimental framework shall investigate the scattering of the elastoresistive behavior when subjected to high load cycle numbers. Furthermore, the spatial homogeneity of the deterioration of the electrical properties of the sensor material shall be addressed.

References

1. Adler, A., Guardo, R.: Electrical impedance tomography: regularized imaging and contrast detection. *IEEE Trans. Med. Imaging* **15**(2), 170–179 (1996). <https://doi.org/10.1109/42.491418>
2. Adler, A., Dai, T., Lionheart, W.: Temporal image reconstruction in electrical impedance tomography. *Physiol. Meas.* **28**, S1–S11 (2007). <https://doi.org/10.1088/0967-3334/28/7/S01>
3. Adler, A., Lionheart, W.R.B.: Uses and abuses of EIDORS: an extensible software base for EIT. *Physiol. Meas.* **27**, 25–42 (2006). <https://doi.org/10.1088/0967-3334/27/5/S03>
4. Bergmayr, T., Winklberger, M., Kralovec, C., Schagerl, M.: Structural health monitoring of aerospace sandwich structures via strain measurements along zero-strain trajectories. *Eng. Fail. Anal.* **126**, 105454 (2021). <https://doi.org/10.1016/j.engfailanal.2021.105454>
5. Cheney, M., Isaacson, D., Newell, J.C., Simske, S., Goble, J.: NOSER: an algorithm for solving the inverse conductivity problem. *Int. J. Imaging Syst. Technol.* **2**(2), 66–75 (1990). <https://doi.org/10.1002/ima.1850020203>
6. Enser, H., Sell, J.K., Hilber, W., Jakoby, B.: Printed strain sensors in organic coatings: in depth analysis of sensor signal effects. *Sens. Actuators A: Phys.* **281**, 258–263 (2018). <https://doi.org/10.1016/j.sna.2018.08.018>
7. Giurgiutiu, V. (ed.): *Structural Health Monitoring with Piezoelectric Wafer Active Sensors*, 2nd edn. Academic Press, Oxford (2014). <https://doi.org/10.1016/B978-0-12-418691-0.00006-X>
8. Graham, B.M., Adler, A.: Objective selection of hyperparameter for EIT. *Physiol. Meas.* **27**(5), S65–S79 (2006). <https://doi.org/10.1088/0967-3334/27/5/s06>
9. Gschoßmann, S., Zhao, Y., Schagerl, M.: Development of data acquisition devices for electrical impedance tomography of composite materials. In: *Proceedings of the 17th European Conference on Composite Materials ECCM17* (2016)

10. Haingartner, M., Gschoßmann, S., Cichocki, M., Schagerl, M.: Improved current injection pattern for the detection of delaminations in carbon fiber reinforced polymer plates using electrical impedance tomography. *Struct. Health Monit.* (2021). <https://doi.org/10.1177/1475921720972308>
11. Katsikeros, C., Labeas, G.: Development and validation of a strain-based structural health monitoring system. *Mech. Syst. Sig. Process.* **23**(2), 372–383 (2009). <https://doi.org/10.1016/j.ymssp.2008.03.006>
12. Kralovec, C., Schagerl, M.: Review of structural health monitoring methods regarding a multi-sensor approach for damage assessment of metal and composite structures. *Sensors* **20**(3) (2020). <https://doi.org/10.3390/s20030826>
13. Loh, K.J., Hou, T.C., Lynch, J.P., Kotov, N.A.: Carbon nanotube sensing skins for spatial strain and impact damage identification. *J. Nondestr. Eval.* **28**, 9–25 (2009). <https://doi.org/10.1007/s10921-009-0043-y>
14. Loyola, B., Arronche, L., LaFord, M., La Saponara, V., Loh, K.: Evaluation of the damage detection characteristics of electrical impedance tomography. In: *ASME 2013 Conference on Smart Materials, Adaptive Structures and Intelligent Systems, SMASIS 2013*, vol. 2, September 2013. <https://doi.org/10.1115/SMASIS2013-3317>
15. Mao, H., et al.: Fatigue damage detection and location of metal materials by electrical impedance tomography. *Results Phys.* **15**, 102664 (2019). <https://doi.org/10.1016/j.rinp.2019.102664>
16. Mitra, M., Gopalakrishnan, S.: Guided wave based structural health monitoring: a review. *Smart Mater. Struct.* **25**(5), 053001 (2016). <https://doi.org/10.1088/0964-1726/25/5/053001>
17. Montgomery, H.C.: Method for measuring electrical resistivity of anisotropic materials. *J. Appl. Phys.* **42**(7), 2971–2975 (1971). <https://doi.org/10.1063/1.1660656>
18. Nonn, S., Schagerl, M., Zhao, Y., Gschossmann, S., Kralovec, C.: Application of electrical impedance tomography to an anisotropic carbon fiber-reinforced polymer composite laminate for damage localization. *Compos. Sci. Technol.* **160**, 231–236 (2018). <https://doi.org/10.1016/j.compscitech.2018.03.031>
19. dos Santos, C.A.M., et al.: Procedure for measuring electrical resistivity of anisotropic materials: a revision of the montgomery method. *J. Appl. Phys.* **110**(8), 083703 (2011). <https://doi.org/10.1063/1.3652905>
20. Tallman, T., Smyl, D.: Structural health and condition monitoring via electrical impedance tomography in self-sensing materials: a review. *Smart Mater. Struct.* **29** (2020). <https://doi.org/10.1088/1361-665X/abb352>
21. Wagner, J., Gschoßmann, S., Schagerl, M.: On the capability of measuring actual strain values with electrical impedance tomography using planar silkscreen printed elastoresistive sensors. *IEEE Sens. J.* **21**(5), 5798–5808 (2021). <https://doi.org/10.1109/JSEN.2020.3036736>
22. Winklberger, M., Kralovec, C., Humer, C., Heftberger, P., Schagerl, M.: Crack identification in necked double shear lugs by means of the electro-mechanical impedance method. *Sensors* **21**(1) (2021). <https://doi.org/10.3390/s21010044>
23. Zhao, Y., Gschossmann, S., Schagerl, M., Gruener, P., Kralovec, C.: Characterization of the spatial elastoresistivity of inkjet-printed carbon nanotube thin films. *Smart Mater. Struct.* **27**(10), 105009 (2018). <https://doi.org/10.1088/1361-665x/aad8f1>
24. Zhao, Y., Schagerl, M., Gschossmann, S., Kralovec, C.: In situ spatial strain monitoring of a single-lap joint using inkjet-printed carbon nanotube embedded thin films. *Struct. Health Monit.* **18**(5–6), 1479–1490 (2019). <https://doi.org/10.1177/1475921718805963>